



**HAL**  
open science

# Numerical and experimental approach for improving quasi-static and fatigue testing of a unidirectional CFRP composite laminate

Fabrizio Pagano, Pascal Paulmier, Myriam Kaminski, Alain Thionnet

## ► To cite this version:

Fabrizio Pagano, Pascal Paulmier, Myriam Kaminski, Alain Thionnet. Numerical and experimental approach for improving quasi-static and fatigue testing of a unidirectional CFRP composite laminate. *Procedia Engineering*, 2018, 7th International Conference on Fatigue Design, Fatigue Design 2017, 29-30 November 2017, Senlis, France, 213, pp.804-815. 10.1016/j.proeng.2018.02.076 . hal-01758746v2

**HAL Id: hal-01758746**

**<https://minesparis-psl.hal.science/hal-01758746v2>**

Submitted on 4 Apr 2018

**HAL** is a multi-disciplinary open access archive for the deposit and dissemination of scientific research documents, whether they are published or not. The documents may come from teaching and research institutions in France or abroad, or from public or private research centers.

L'archive ouverte pluridisciplinaire **HAL**, est destinée au dépôt et à la diffusion de documents scientifiques de niveau recherche, publiés ou non, émanant des établissements d'enseignement et de recherche français ou étrangers, des laboratoires publics ou privés.



7<sup>th</sup> International Conference on Fatigue Design, Fatigue Design 2017, 29-30 November 2017,  
Senlis, France

## Numerical and experimental approach for improving quasi-static and fatigue testing of a unidirectional CFRP composite laminate

Fabrizio PAGANO<sup>a,b</sup>, Pascal PAULMIER<sup>a</sup>, Myriam KAMINSKI<sup>a</sup>, Alain THIONNET<sup>b</sup>

<sup>a</sup>ONERA The French Aerospace Lab, 29, avenue de la Division Leclerc, 92322 Châtillon, France

<sup>b</sup>Ecole Nationale Supérieure des Mines de Paris – Centre des Matériaux P.M. Fourt – UMR CNRS 7633 – BP 87, 91003 Evry Cedex, France

---

### Abstract

Mechanical response of CFRP unidirectional prepreg was investigated under tensile quasi-static and fatigue loading. Firstly, the findings of an initial investigation on the effects of the end tabs and gripping condition are presented. A dialogue between numerical simulations and experimental tests led to avoid premature splitting failures in the clamps. Proper tensile failure is assessed in the gage length, at enhanced strength levels for the material considered. Consequently, the unidirectional material was successfully tested under tension-tension fatigue, at high load levels. Fatigue damage mechanisms arise at high stress amplitude, revealing that also a UD laminate can suffer from fatigue degradation along the fibres direction.

© 2018 The Authors. Published by Elsevier Ltd.

Peer-review under responsibility of the scientific committee of the 7th International Conference on Fatigue Design.

*Keywords:* CFRP composites; mechanical testing; tensile strength ; stress concentration; gripping pressure; fatigue.

---

### 1. Introduction

In a multidirectional carbon fibres reinforced plastic (CFRP) composite laminate, the longitudinal plies govern the fatigue life performance of the laminate in most cases. These plies have long continuous fibres aligned with the load direction, thus the fibres give almost the entire contribution of the stiffness and strength of the ply. In order to predict the fatigue life of a multidirectional composite laminate it is therefore necessary to have a good estimation of the tensile strength and the fatigue behavior of the unidirectional (UD) plies, under uni-axial tension load along the fibres direction (0°). The identification of these basic mechanical properties requires extremely difficult tests: because of the high anisotropy of the material, splitting (shear failure of the matrix) parallel to the fibres takes place prior to tensile rupture. This damage mode initiates at the end of the clamped region of the specimen, leading to an abrupt brittle explosive failure outside the gage length, as showed in [1,2]. Hence, the validity of the test is severely affected and the effective tensile strength could be underestimated.

The ASTM D3039/D3039M and ISO 527-1 standards test method for quasi-static tensile properties of CFRP composites suggest the use of tabs to provide a soft interface. The material can be aluminium, or a E-glass fibre reinforced plastic composite, in a  $[0/90]_{ns}$  laminate configuration. The composite tab is commonly applied at  $45^\circ$  to the loading direction. Both standards recommend a tab length of at least 50 mm. The adoption of a tapered geometry for the tabs, with low bevel angle ( $7^\circ$  to  $10^\circ$ ) is proposed but not compulsory. The grips should overhang the end of the tabs by about 10 mm. No quantitative indications are given concerning the clamping pressure. Finally, the specimen must be rectangular shaped, because the dog-bone geometry induces spurious premature failure characterized by splitting along the fibres direction. These standards give only recommendations, and no definitive solution is stated to avoid the premature failure in the clamping region.

In literature, there are few articles on the subject [2-9]. In most cases, numerical studies are proposed on the tabs design, through FEM models. The influence of several parameters is analyzed and compared: tab material, tab bevel angle, tab thickness, clamping configuration and pressure. In authors' knowledge, no unique and definitive solutions fully supported by experimental findings seem to be achieved.

When performing fatigue tests, clamping failure is even more likely to occur. The ASTM D3749/D3749M standard test method for tension-tension fatigue of CFRP composites adopts the same recommendations as the ASTM D3039/D3039M. Bibliography contains very rare studies on fatigue tensile tests along the fibres direction. A common belief, widespread in scientific community, states about the absence of fatigue phenomena in unidirectional CFRP laminates, when loaded in the fibres direction; hypothesis supported by nearly horizontal SN curves. In fact, carbon fibers are elastic in behavior and have been demonstrated not to suffer from fatigue failure [10]. However, firstly, fibres strength properties present a Weibull probability distribution. Secondly, micro-tomography observations in [11] showed the existence of large fibres break accumulation in clusters, prior to final failure, at high percentage of the ultimate load of a unidirectional ply. Thirdly, in a composite, fibers are embedded in the matrix, within a non-regular distribution. Thus the composite can suffer from a fatigue process by damage or degradation of the matrix and of the fibre interface, and by the acceleration of the fibres breaks clusters accumulation.

These fatigue phenomena into unidirectional CFRP laminates arise only at very high stress levels; but it is extremely difficult to achieve these experimental conditions, because of premature failure problems.

In [5], an original testing apparatus allowed to successfully test a T700/epoxy unidirectional specimen, without producing stress concentration in the clamps. It has been demonstrated the existence of fatigue degradation phenomena at high cyclic load levels and amplitude. However, the testing apparatus is difficult to realize and the UD specimens were cut from a thin pultruded material. The extensions of the achieved results to UDs and multidirectional thicker prepregs, typically used in aerospace industry, cannot be directly deduced.

The objective of this paper is to illustrate the authors' findings in investigation on the tensile strength and fatigue behavior of a UD CFRP with long continuous carbon fibres, under uni-axial tension load.

Firstly, we show results achieved in setting up a procedure and a testing apparatus that conduced to a proper tensile failure. Investigations are based on a numerical and experimental dialogue. A valid failure has been obtained at enhanced strength levels compared to strength values generally found in the literature for the considered material. Secondly, on the basis of the proposed testing procedure, experimental tests have been led under cycling loading and have shown that fatigue degradation at high stress amplitude and load level can occur for a UD CFRP laminate.

## **2. Materials and equipment**

### *2.1. Specimen and tabs materials*

The unidirectional laminates used in this study are made from Toray T700GC/M21 prepregs, 57 % of fibre volume. Stacking sequences of four, eight, and sixteen plies were tested. Experimental tests found in the literature identified UTS (ultimate tensile strength) values between 1900 and 2200 MPa for this material [12, 13]. In this study, the choice has been made to use an indicative value of  $X_t = 2000$  MPa as reference for the first numerical simulations. The engineering constants used in the FEM model derive from identification works carried out in [12, 13], and are summarized in Table 1.

Table 1. In-plane elastic properties of specimen and tabs materials tested, and used in FEM simulations.

	Specimen		Tabs	
	T700GC/M21 UD laminate	E-glass fibres/RTM6 woven	Aluminium	
Longitudinal modulus ( $E_l$ )	115000 MPa	42150 MPa	70000 MPa	
Transverse modulus ( $E_t$ )	8500 MPa	10235 MPa	70000 MPa	
Shear modulus ( $G_{lt}$ )	9000 MPa	3760 MPa	26315 MPa	
0° Tensile strength ( $X_T$ )	1900 MPa	-	-	
90° Transverse tensile strength ( $Y_T$ )	84 MPa	-	-	
Shear strength ( $S_T$ )	75 MPa	-	-	
Thickness	0.264 mm (ply)	0.25 (ply)	3 mm (total)	

The tabs were cut from 3 mm aluminium sheets, and from a 12-ply E-glass fibres/RTM6 equilibrated woven (Table 1). They were bonded to specimens with Araldite 2011 glue.

### Experimental setup

All tests were performed at standard atmospheric condition, on a servo hydraulic MASER testing machine, 500 kN capacity, equipped with hydraulic wedge grips. The maximum allowable gripping length is 85 mm. In order to have the 10 mm gap between the grips and the tabs end, suggested by ASTM D3039, a gripping length of 75 mm was initially adopted. During tension tests, specimens were subjected to monotonic tensile loading with a rate of 2 mm/min.

Specimens were instrumented by stereo-digital image correlation (DIC) to measure stress-displacements curve, get the elastic moduli, and verify the good alignment of the specimen along the tensile axis; the SENSICAM cameras have 2048 x 2048 pixels resolution.

Two acoustic emissions MISTRAS sensors were fixed at the borders of the gage length of the specimen, to detect and isolate the real damage (fibre breaks) from the noise and damage coming from the clamped region.

By means of an infrared high-frequency FLIR camera, passive thermography is used to measure global specimen heating and to detect hot damage spots in the surface specimen.

## 3. Preliminary numerical analysis

A series of initiatory numerical analysis were carried out through a finite element model, simulating the quasi-static uni-axial tension test, and involving different tabs configurations. The purposes here are:

- understand the physical mechanisms that induce premature splitting failures in the tab region;
- discern main trends and influence of several design parameters, and verify that our test cases are in agreement with literature findings;
- correlate results with laboratory tests illustrated further.

### 3.1. Modeling of the tension test

Meshes and calculations are realized with ZeBuLoN™. Only linear elastic simulations were performed. Figure 1 illustrates the simulated parts in the finite element model, along with symmetry and boundary conditions. Because of symmetry, only a quarter of the layout is modeled.

The specimen is a  $[0^\circ]_{16}$  of T700GC/M21 (elastic properties illustrated in Table 1). According to ASTM D3039, it has a rectangular shape, with a gauge length of 140 mm and a minimal tabbed length of 55mm (for rectangular tabs).

Both aluminium tabs and 12 plies GFRP tabs have been modeled (Table 1). The tabs thickness is 3 mm. Several bevel angles are tested. In each geometric configuration, the gripping area, i.e. the superior face of the tab where external load is applied, has a length of 55 mm (ASTM D3039). The authors made the choice to keep constant the gripping length and the gauge length of the specimen, in order to perform proper comparisons. Therefore, the overall length and the tabbed length of the specimen vary in function of the tab bevel angle.

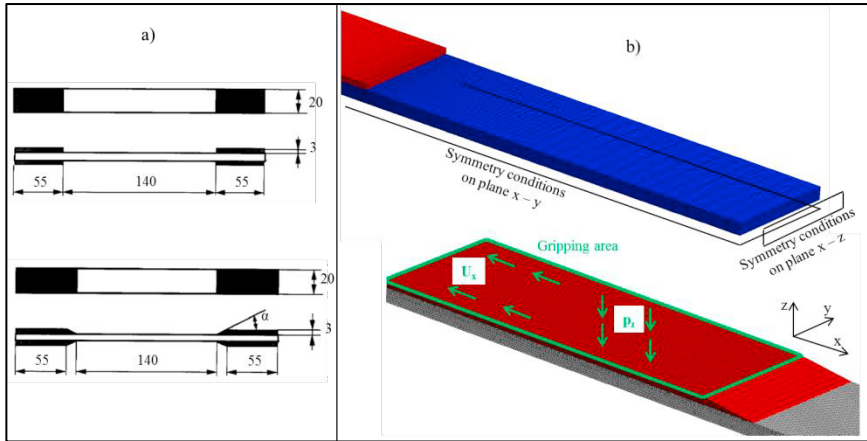


Figure 1.a) Specimen geometries used in the FEM model (dimensions in mm).  
 b) Boundary conditions of the FEM model.

Since it is a preliminary analysis, no glue or any interface layer is modeled between tabs and the specimen: the two components are perfectly bonded in the mesh. All parts were meshed with quadratic brick elements.

The clamps were not simulated in the finite element model; the reader can refer to [6] for more details about wedge grips and contacts conditions simulation. The external load is applied on the gripping area. A pressure is imposed along the z axis, and a uniform negative displacement acts along the x axis (respectively \$p\_z\$ and \$U\_x\$ in Figure 1). Initially \$U\_x\$ is chosen in such a way that the central part of the gage length reaches a longitudinal stress of 1500 MPa. This value being far from the supposed tensile strength of the material (2000 MPa), the hypothesis of a linear elastic model without damage keeps its validity. An indicative value of 20 MPa has initially chosen for \$p\_z\$. In practice, as explained further in paragraph 4., the testing machine applies a much bigger pressure; however we preferred at the first stage to keep a lower value in order to isolate and identify the effects of the different parameters. Finally, y-displacements are blocked on the gripping area.

### 3.2. Comparative results and influence of the main parameters

Figure 2 gives an overview of the simulation with rectangular aluminium tabs. Each component of the stress tensor presents a high peak exactly behind the end of the tab. This peak takes place in a localised region of the upper ply of the specimen, close to the surface. Particular attention must be given to transverse and shear stress components, \$\sigma\_{22}\$ and \$\sigma\_{12}\$. Actually, they are responsible for splitting damage mode. A criterion has been used to study the combined effect of these stresses [13]:

$$f2_+ = \left(\frac{\sigma_{22}}{Y_t}\right)^2 + \left(\frac{\sigma_{12}}{S_c(1-p\sigma_{22})}\right)^2 \tag{1}$$

The reader can refer to [13] for more details about the formulation and the constants of this criterion.

The positive values of \$\sigma\_{22}\$ and \$\sigma\_{12}\$ are caused by a constrained Poisson effect. The coupon tries to compress transversely because it is under longitudinal tension. The tab prevents this process, and by reaction there is a positive transverse tension and shear in the specimen. The UD has extremely low transverse strength properties. The high values of the stress intensity factors explain the premature failure of the specimen in the tabbed region.

An important remark must be made about the interpretation of the results: the peak stress observed in Figure 2 is due to a singularity in the model. Since it is a finite element model, the peak itself and the related stress intensity factors strongly depend on the mesh refinement. Furthermore, the implemented material law is linear elastic.

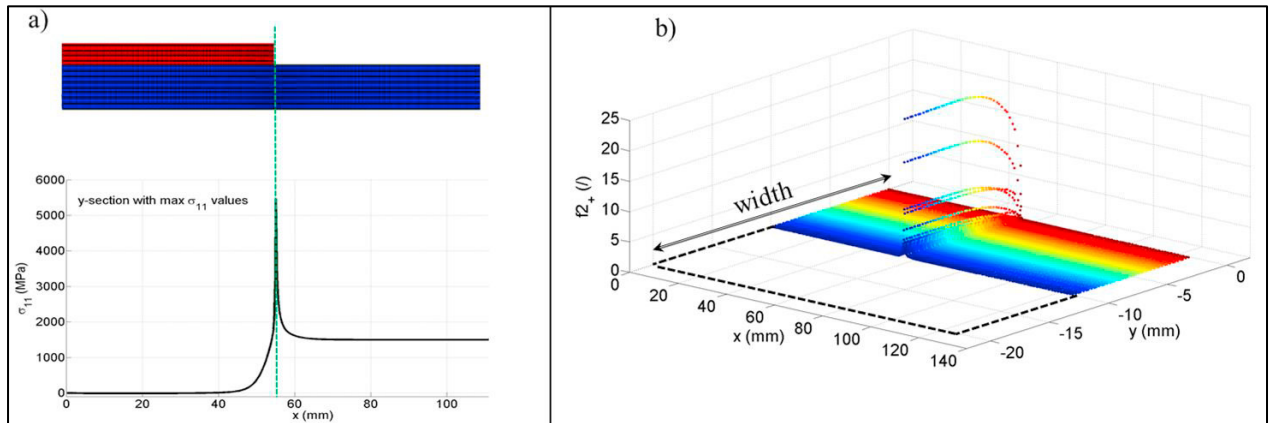


Figure 2. a) Longitudinal stress  $\sigma_{11}$  along the middle  $y$ -section on the surface of the specimen with rectangular aluminium tabs. b) 3D plot of the  $f_{2+}$  criterion on the surface specimen for the same configuration.

The presented results are only qualitative and must be interpreted only in terms of comparisons between two or more configurations, in order to understand which one is more advantageous and to discern main tendencies. Hence, the same mesh refinement has been used in the end tabs region for all the simulated configurations.

Figure 3a) shows the comparison between specimens with rectangular aluminium tabs, and GFRP tabs. Components of the stress tensor are plotted along a specific  $y$ -section of the coupon, on the surface of the specimen. The  $y$ -section plotted is that one where the maximum value of the stress peak is reached. For example, in the case of a specimen with rectangular aluminium tabs, the maximum value of  $f_{2+}$  is reached in the middle  $y$ -section, as illustrated in the 3D-plot of Figure 2 b).

It must be noted that sometimes the section with the highest peak of some shear components is situated close the lateral edges of the specimen. That may explain a lateral premature splitting, showed in Figure 4, encountered in the first tests illustrated further in paragraph 4.

As could be expected, the stress concentrations are the highest for the metallic tabs. This could be explained because of a higher stiffness of the material, which does not allow a sufficient smooth load transfer from tabs to the coupon. The stacking sequence of the GFRP tabs is  $[+45^\circ/-45^\circ]_6$ , as prescribed by standards. A  $[0^\circ/90^\circ]_6$  configuration has been also simulated. However, the previous orientation showed better results, because it provides a softer interface. Simulation results are not showed for the sake of synthesis. In the following simulations, only the  $[+45^\circ/-45^\circ]$  stacking sequence has been used for the GFRP tabs.

The use of long tapered tabs induces large decrease in stress concentrations, as showed in Figure 3b). A bevel angle of  $7^\circ$  has been modeled for the tabs, as it is the minimum value suggested by the standards. These tabs redistribute the load gradually. Two peaks of stresses appear now in the surface specimen along the  $x$  direction. The biggest one takes place at the end of the gripping length (superior tab tip), the second one occurs at the end of the tabbed length (inferior tab tip). The overall intensity of the stresses at the tabs tips is vastly reduced, and the differences in terms of stress intensity factors between tabs with different materials is reduced as well.

In agreement with literature, the tab angle has demonstrated to be an important design parameter in this study. Thus, a series of simulations have been done using aluminium tabs with different bevel angles. The maxima values of the  $f_{2+}$  criterion are plotted in Figure 5. Components of the stress tensor have similar trends. Length is normalised because specimens with different tapered tabs have different overall length.

Numerical investigations have been done with different tab thicknesses. A slight diminution of the peak stress in the coupon was observed with the increase of the thickness. Findings are in agreement with [9], where more details

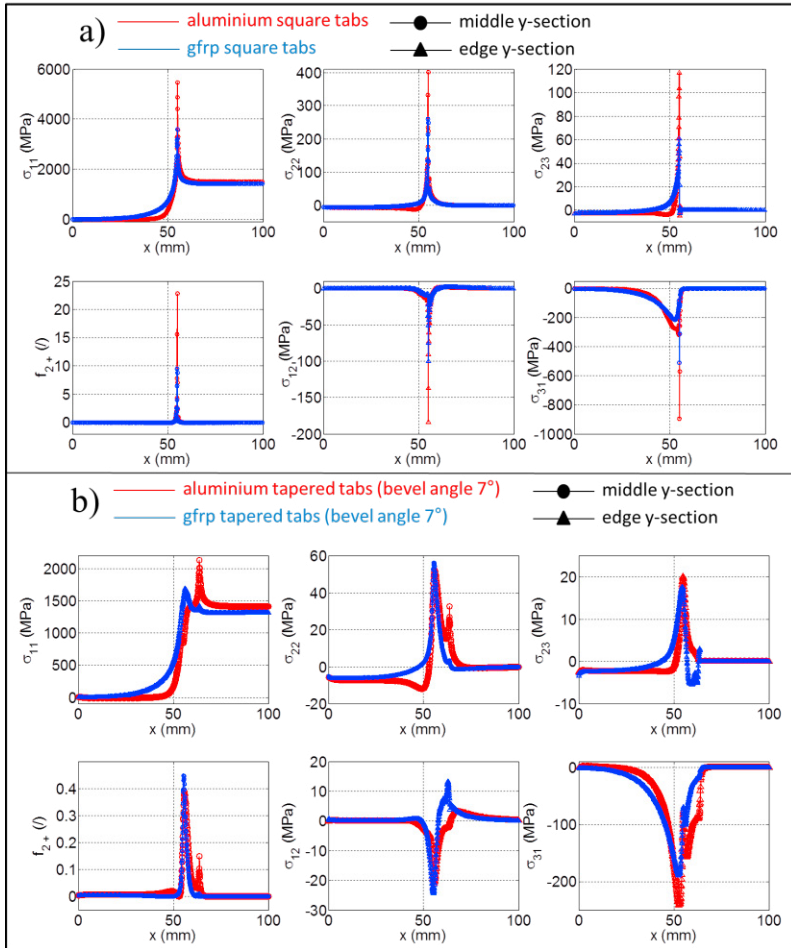


Figure 3. Evolution of the components of the stress tensor along the surface of the specimen. y-section corresponding to the highest stress concentration factors.

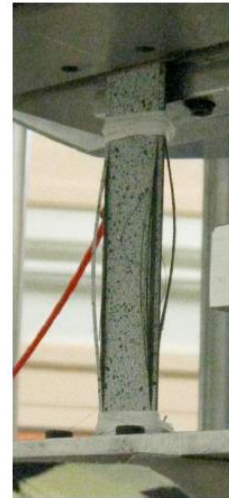


Figure 4. Lateral splitting observed in experimental tests, prior to final failure.

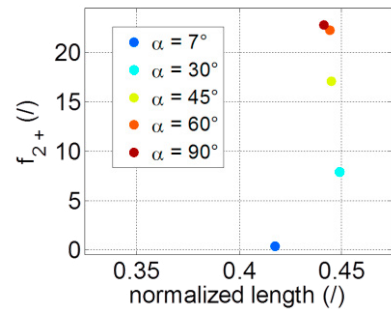


Figure 5. Evolution of the maximum value of  $f_{2+}$  criterion on the surface specimen, in function of the tab bevel angle. Aluminium tabs.

are given. Finally, the gripping pressure was not the object of a parametrical analysis because it is not a free parameter: being applied by the machine as directly linked to the axial force to exercise, it is given by machine specifications.

#### 4. Preliminary quasi-static tests

##### 4.1. Misalignment angle

Tension tests on UD along the fibres direction are very sensible to the alignment angle between the specimen itself and the load axis. Because of the high anisotropy of the material, a little misalignment angle can lead to splitting failure piloted by the  $f_{2+}$  criterion, prior to a proper tensile failure piloted by the tensile strength of the material. An attempt to evaluate this critical angle has been performed though an analytical study. The  $f_1$  criterion is given by the tensile applied stress  $\sigma_{11}$ , divided by the UTS ( $X_t$ , Table 1). The components  $\sigma_{11}$ ,  $\sigma_{22}$  and  $\sigma_{12}$  become dependent of the introduced misalignment angle  $\Theta$ . Therefore  $f_1$  and  $f_{2+}$  vary in function of  $\Theta$ . As illustrated in Figure 6, the critical angle is around  $2^\circ$  for the material considered in this study: beyond this value, premature failure

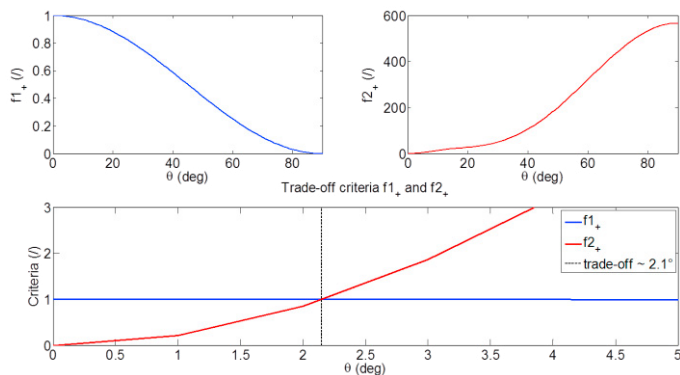


Figure 6. Trade-off between  $f1_+$  and  $f2_+$  for the critical misalignment angle.

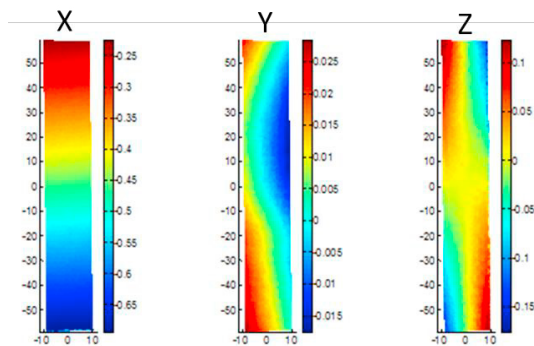


Figure 7. Asymmetric displacement fields introduced by the presence of a misalignment angle between the specimen and the traction axis. (Values in colorbars are expressed in mm).

induced by splitting is likely to take place before tensile failure. DIC was used during the tests to analyse the displacements fields. Figure 7 shows an example of an excessive misalignment angle introduced in the experimental setup, which should be avoided.

Another source of misalignment angle appears when the specimen is not cut perfectly parallel along with the fibres direction. This may induce lateral splitting showed in Figure 4. In this latter case, the authors can only suggest to pay particular attention when cutting the specimens.

#### 4.2. Clamping Force

The clamping force to be applied by the hydraulic wedges is directly related to the axial force needed to test the specimen. This relation is given as a specification of the testing machine. Figure 8 presents a curve extracted from the user manual of the testing machine used. The clamping force is actually expressed in terms of the pressure to apply to the pistons acting on the wedges. Similar curves are given for any other testing machine.

The first series of experimental test is effectuated on  $[0^\circ]_{16}$  specimens. The force to apply is obviously dependent of the section of the specimen (thickness per width).

Since the clamping force is not a free parameter, in order to minimize the pressure acting on the gripping area of the coupon, the gripping area itself should be maximized. This area is given by the width per the gripping length. Increasing the width would lead to an augmentation of the needed axial force. Therefore, the only parameter to optimize is the gripping length: the authors suggest designing tabs that are as long as the clamps length, in order to maximize the gripping length.

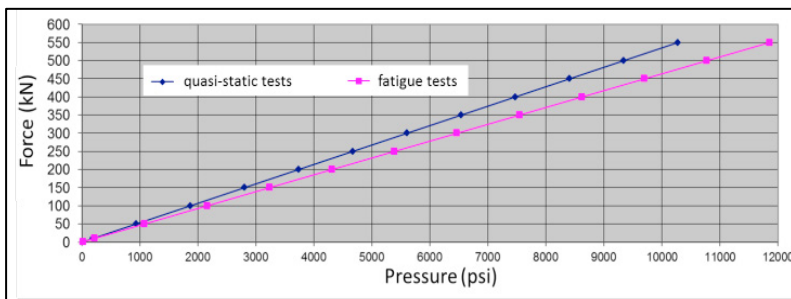


Figure 8. Relation between the axial force to apply and the clamping force required, for the 500 kN MASER testing machine.

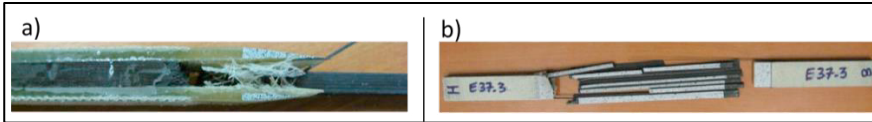


Figure 9. Examples of premature failures.

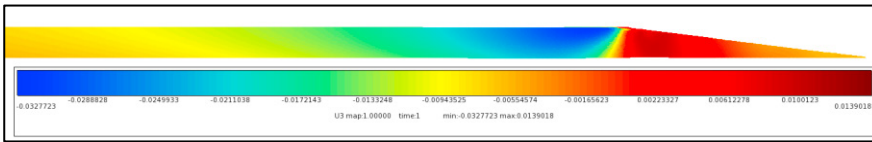


Figure 10. Distribution of the z-displacements of the GFRP tab, 10° bevel angle. Numerical simulation of the traction test (values in mm).

### 4.3. Premature failures

Both square tabs and tabs with 10° bevel angle were used, made of aluminium and of GFRP composite (Table 1) for the experimental tests. The length of the superior face of the tabs was 75mm, i.e. the maximum allowable gripping length. Tabs were 3mm thick. The value of required pressure on the gripping area was known to be a bit less than 180 MPa for  $[0^\circ]_{16}$  coupons. Several attempts were made to reduce this value without encountering slipping problems. Barely 20 MPa were gained.

In each test where tapered tabs were used, the beveled region of the tab detached from the specimen, prior to final failure as shown in Figure 9a). A characteristic acoustic signature, detected by the acoustic sensors, made possible the identification of the detachment during the tests.

Indeed, even if debonding is not possible in the FEM model, numerical simulations show positive displacements of the beveled part of the tab along the z-axis (Figure 10). Firstly, this part is not in contact with the clamps; thus, no pressure is applied there to ensure the contact with the specimen. Secondly, only the specimen is subjected to transversal compression due to the Poisson effect. It can be deduced that the adhesive layer cannot withstand these singularities, resulting in the separation of the end part of the tabs. Therefore, the advantages of having long tapered tabs to provide a smooth load transfer cannot be exploited.

Each specimen has presented spurious premature failures, at values around 2000 MPa (Figure 14). In the cases where beveled tabs were used, a tensile rupture took place in the tab region at the point where the debonding between the tabs and the specimens ends, as illustrated in Figure 9a). The peak of  $\sigma_{11}$ , which in previous simulations was shown to be situated at the end of the gripping length (3.2), cannot be smoothed by the tapered portion. In most cases, with rectangular or oblique tabs, splitting has also occurred, as observed in Figure 9b).

## 5. Improved quasi-static tests

The best way to reduce the clamping pressure is to reduce the thickness of the laminate. A new series of numerical simulations has been realized, modeling a  $[0^\circ]_4$  laminate. Figure 11 shows a comparison between the 4-ply and the 16-ply FEM model. Instead of imposing the same value of the negative  $U_x$  displacement, two different values have been chosen, in such a way that the two specimens reach the same tensile stress  $\sigma_{11}$  in their gage length. The chosen stress is the maximum value of UTS recorded during the first series of experimental tests. The  $U_x$  displacement needed for the thinner laminate is smaller, i.e. less force is needed to reach failure. Then, a lower value of clamping force is required. Comparative results in Figure 11 show much lower stress concentrations for the thinner laminate, even if both specimens reach the same longitudinal stress in their gage length.

On the basis of these simulations outcomes, two new batches of specimens were fabricated and tested, made of eight and four plies. Only square tabs were used. Thanks to thinner sections, a substantial reduction of the required pressure on the gripping area is achieved. It was possible to decrease the pressure till 62 MPa for  $[0^\circ]_4$  laminate, without encountering slipping problems. Two beneficial effects were obtained. Firstly, an important augmentation of the tensile strength was observed. Secondly, for the lower values of clamping pressure applied on the

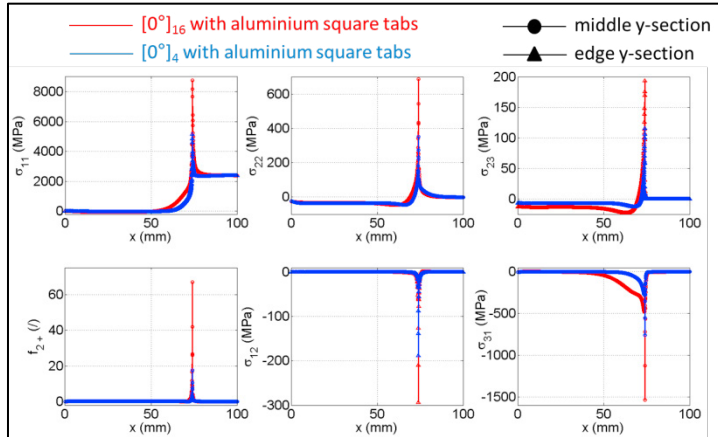


Figure 11. Evolution of the components of the stress tensor, along the surface of the specimen. y-section corresponding to the highest stress concentration factors. Comparison between  $[0^\circ]_4$  and  $[0^\circ]_{16}$  laminate.

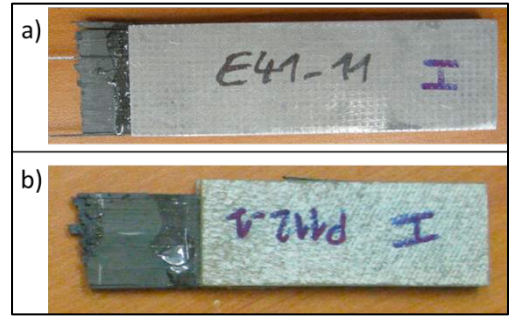


Figure 12. Proper tensile failure on UD specimens, with aluminium (a) and GFRP (b) square tabs.

$[0^\circ]_4$  specimen specimens, a proper tensile failure took place in the gage length, without splitting, as showed in Figure 12. A net failure occurs, in the gage length, perpendicular to the longitudinal axis and extended along all the width. Then, an extremely rapid dynamic process follows and causes the violent explosion of the specimen. The final failure is so fast, that it is not generally possible to capture it even with the high-frequency infrared camera, settled at 200 Hz acquisition frames. It was possible to detect a hot-spot on the surface of the specimen only in one case, just before the final failure (Figure 13). The damage onset took place in the central gauge length. Then it propagated very fast along the longitudinal direction, and in a few tenths of a second the failure of the specimen occurred as showed in Figure 12a).

Figure 14 summarizes all the experimental tension tests carried out in this study. An evident relation can be observed between the augmentation of the tensile strength, and the reduction of the number of plies, along with the clamping pressure. This trend seems to stabilize to an asymptotic value of 2600 MPa, where the differences between specimens equipped with different tabs materials are negligible.

One coupon failed at 2400 MPa: an atypical failure surface was observed, extended partly in the gage length, and partly at the tab tips. Only one specimen failed at a value greater than 2600 MPa: this value deviates from the general trend illustrated in Figure 14, and it has a significant distance from other values.

Finally, it seems pertinent to consider the value of 2600 MPa as the real UTS of the material. The three specimens failed around this value, with a clamping pressure of 60-80 MPa, have showed a proper tensile failure.



Figure 13. Hot-spot identified by passive thermography on the surface of a  $[0^\circ]_4$  specimen, shortly before the tensile failure.

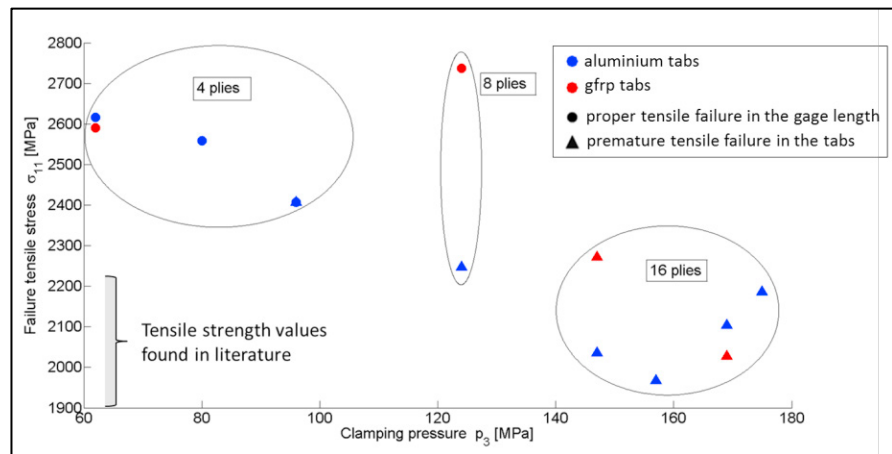


Figure 14. Summary of the tension tests realised on the UD  $[0^\circ]_n$  laminates. On the abscissa are reported the values of the needed clamping pressure, acting on the gripping area of the specimen. The corresponding failure strengths achieved are showed on the y-axis.

## 6. Fatigue tests

No numerical simulations of fatigue tests were conducted. However, some considerations can be deduced from the simulations of the quasi-static test exposed in 3. As stated in 3.2, the transverse and shear stresses, mainly responsible for splitting, are due to a contrasted Poisson effect, induced by the presence of a longitudinal stress,  $\sigma_{11}$ . If the specimen is subjected to a cyclic tension loading, i.e.  $\sigma_{11}$  has a cyclic variation, the other stress components also undergo a cyclic variation. This process of “fatigue” clamping-induced load makes the premature failure of the specimen even more likely to happen.

Six fatigue tests, performed under load controlled conditions, are presented in this study. They are summarized in Table 2. All the specimens were equipped with square aluminium tabs. This choice is motivated by the following considerations:

- from the experimental outcomes illustrated in 4. and 5., no evident benefit is conferred by the use of (i) tapered tabs and (ii) GFRP composite tabs;
- an accurate analysis of acoustic emissions on previous tests indicates the presence of considerable noise coming from the GFRP tabs. The associated acoustic signature cannot be distinguished from the real damage of the specimen (mostly fibres ruptures). On the contrary, aluminium tabs produce almost no acoustic events.
- in [8], thermal analyses of specimens’ edges under cyclic loading are showed. Different tabs solutions are compared. Aluminium tabs reduce the most the heating peak localized at the end of the tabbed region, if compared to the GFRP tabs, and induce a more gentle transition from gripped to free length.
- cutting of square aluminium tabs is a time and cost saving solution.

As described in [5], evident degradation in long continuous carbon fibres UD composites arises only at sufficiently high load levels and amplitude. Then, the aim is to fatigue the coupons at 80-90% of their tensile strength, identified in quasi-static tests. Being aware of the splitting failures occurring at around 2000 MPa for thicker laminates, a maximum stress level of 1700 MPa was imposed to the two 16-ply specimens. Two different stress ratios were performed, in order to evaluate the influence of the stress amplitude. The cyclic frequency was 3Hz.

The  $[0^\circ]_{16}$  specimen was solicited at  $R=0.5$  during 50.0000 cycles and did not break. No macroscopic visible damage was observed when the test was stopped. The surface of the specimen was observed by SEM. Both isolated broken fibres and clusters of broken fibres were observed, as showed in Figure 15. Little matrix cracking seemed to propagate from the crack surfaces of the broken fibres. The biggest cluster observed was composed of three fibres. The stress level imposed is only the 65% of the supposed real tensile strength of the material, i.e. 2600 MPa. Though the considerable fibre failures disseminated on the surface may evidence the beginning of a damage process, the applied fatigue load has demonstrated to be too low to lead to a macroscopic degradation of the material.

The  $[0^\circ]_{16}$  specimen fatigued at  $R=0.1$  broke after almost 23.000 cycles by splitting in the tabbed region. No conclusion can be made on this test because of the spurious failure reported outside the gage length.

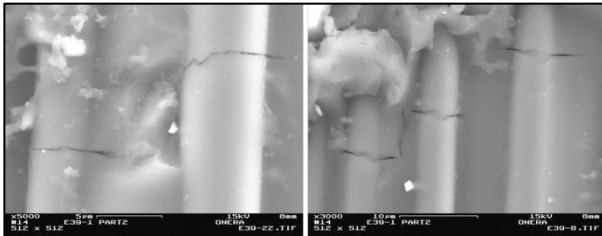
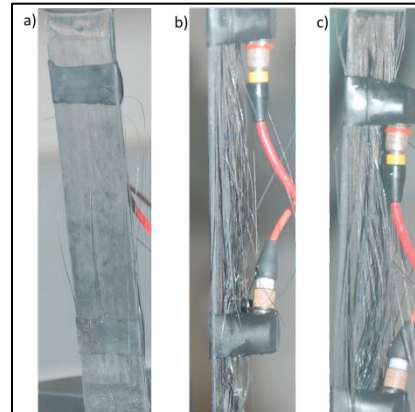
The augmentation of the mean temperature recorded with an infrared camera in both fatigue tests was less than  $10^\circ\text{C}$ , which is the warning limit for overheating as suggested by the standard ASTM D3479. Consequently, the cycle frequency was increased up to 5 Hz to realize the tests on the  $[0^\circ]_4$  specimens. No heating difference was observed between these latter tests and the previous ones performed at 3 Hz.

The use of thinner coupons made possible to increase the maximum stress level up to 2300 MPa without inducing premature failures. The two fatigue tests performed with a stress ratio  $R=0.5$  induced no failure after 50.000 cycles and 100.000 cycles, as well as the previous test with the thicker laminate, interrupted at 50.000 cycles. A monotonic tension load has been applied until failure to the specimen E41-3 (Table 2): a proper tensile failure took place in the gage length at 2553 MPa. This value stands inside the incertitude range associated to the tensile strength (Figure 14). It seems that the applied fatigue load induced no manifest degradation of the material after 50.000 cycles.

Another scenario took place when a stress ratio of  $R = 0.1$  was applied to a  $[0^\circ]_4$  specimen, subjected to  $\sigma_{\text{MAX}}=2300$  MPa. A progressive macroscopic degradation severely affected the coupon E41-4, starting at around 5.000 cycles. Figure 16 shows a progressive unusual damage process: fibres or bundle of fibres pull out dissociating

Table 2. Fatigue tension-tension tests conducted on  $[0^\circ]_n$  specimens along the fibres direction.

Specimen	N° plies	R	$\sigma_{MAX}$ (MPa)	f (Hz)	Failure	Residual performance tension test (MPa)
E39-1	16	0.5	1700	3	Run out (50000 cycles)	-
E37-12	16	0.1	1700	3	Splitting @ 22736 cycles	-
E41-3	4	0.5	2300	5	Run out (50000 cycles)	2553
E41-8	4	0.5	2300	5	Run out (100000 cycles)	-
E41-4	4	0.1	2300	5	Tensile rupture @ 26564 cycles	-
E41-6	4	0.1	2300	5	Tensile rupture @ 27406 cycles	-

Figure 15. Examples of fibre breaks observed on the surface specimen (E39-1), after 50.000 cycles at  $R=0.5$ ,  $\sigma_{MAX}=1700$  MPa,  $f=3$  Hz.Figure 16. Fatigue deterioration of the  $[0^\circ]_4$  specimen E41-4, after a) 5.000 cycles, b) 20.000 cycles, c) 25.000 cycles.  $\sigma_{MAX}=2300$  MPa,  $f=5$  Hz.

from the matrix, and breaking. It can be supposed that the high stress amplitude combined with the high stress level, caused an important degradation of the matrix, along with numerous fibre failures. These damages led to a critical deterioration of the structural integrity of the specimen, which induced a final failure at 26.564 cycles. The failure was explosive and broom-like, though it was concentrated in the gage length.

Coherent results were observed for the specimen E41-6, subjected at the same experimental conditions: the progressive damage process illustrated in Figure 16 took place for this latter specimen also, which induced a final failure at 27.406 cycles.

Similar damage process and final failure were observed in [5] with pultruded CFRP UD subjected to high cyclic strain amplitudes.

## 7. Conclusions and Perspectives

A dialogue between numerical simulations and experimental tests allowed identifying the best clamping configuration to test a UD CFRP composite with long continuous fibres, along the fibres direction. Several recommendations can be outlined from this initial study. Square cut aluminium tabs should be used, as long as possible, limited only by the clamps length. The end tabs should be positioned completely between the grips. Mounting the specimen must require very attention to achieve an optimal alignment with the load axis; DIC may help in this task. The clamping pressure found out to be the most influent parameter. It must be minimized. The best way to accomplish that is to reduce the thickness of the specimen.

Once all these precautions have been taken, (i) specimens showed a proper tensile failure, with a net cut in the gage length perpendicular to fibres direction; (ii) a considerable gain was obtained concerning the strength value, and an ultimate tensile strength of 2600 MPa has been reached without premature splitting failures.

The authors should perform more quasi-static tests in the optimized clamping configuration, in order to study the statistical dispersion in the tensile strength of the material.

The know-how acquired in the first part of this study allowed the investigation of the fatigue behavior of this material, along the fibres direction.

The maximum applied stress in fatigue tests on the  $[0^\circ]_{16}$  specimens was only 1700 MPa, which corresponds to 85% of the UTS referenced in the literature. However, it represents only 65% of the UTS reached during the previous quasi-static tests. The test at  $R=0.5$  was stopped at 50.000 cycles. Large number of fibre breaks was observed on the surface, though no macroscopic property degradation of the material seemed to take place. Authors intend to analyze the core of the coupon with micro-tomography, in order to check if the encountered fibre breaks are not due only to a surface effect.

The use of thinner specimens, along with the optimized clamping configuration, made possible to perform fatigue tests at 90% of the UTS reached for this material. It has been shown that the material suffers from a fatigue process if specimens are subjected to sufficiently high stress amplitude, i.e.  $R=0.1$ . Important matrix degradation occurred, plenty of fibres and fibres bundles debonded from matrix and led to failure. The disintegration of the specimens happened at around 25.000 cycles at  $R=0.1$ ; whereas at  $R=0.5$ , (i) the residual performance tension test after 50.000 cycles revealed no strength reduction, and (ii) no failure occurred after 100.000 cycles. That seems to testify an important role played by the stress ratio.

Authors intend to perform more similar fatigue tests in order to confirm the results achieved, and to state about the statistical dispersion that characterizes these experimental data. Detailed analysis of the acoustic emissions and of the passive thermography will be discussed in a forthcoming study.

## Acknowledgements

The authors would like to thank Jean-Christophe Teissedre (Ecole Nationale Supérieure des Mines de Paris, Centre des Matériaux) for his contribution to this study and for having shared his experience on the topic.

## References

- [1] M. Kawai, K. Yano, Anisomorphic constant fatigue life diagrams of constant probability of failure and prediction of P–S–N curves for unidirectional carbon/epoxy laminates, *International Journal of Fatigue*, Volume 83, Part 2, February 2016, Pages 323-334.
- [2] M. Hojo, Y. Sawada, H. Miyairi, Influence of clamping method on tensile properties of unidirectional CFRP in  $0^\circ$  and  $90^\circ$  directions - round robin activity for international standardization in Japan, *Composites*, Volume 25, Issue 8, 1994, Pages 786-796.
- [3] A.K. Green, L. Shikhmanter, Coupon development for fatigue testing of bonded assemblies of pultruded rods, *Composites Part A: Applied Science and Manufacturing*, Volume 30, Issue 5, May 1999, Pages 611-613.
- [4] C.T. Sun, I. Chung, An oblique end-tab design for testing off-axis composite specimens, *Composites*, Volume 24, Issue 8, 1993.
- [5] Y. Meziere, A.R. Bunsell, Y. Favry, J.-C. Teissedre, A.T. Do, Large strain cyclic fatigue testing of unidirectional carbon fibre reinforced epoxy resin, *Composites Part A: Applied Science and Manufacturing*, Volume 36, Issue 12, December 2005, Pages 1627-1636.
- [6] I. De Baere, W. Van Paeppegem, J. Degrieck, On the Design of End Tabs for Quasi-Static and Fatigue Testing of Fibre-Reinforced Composites, *Polymer composites*, 2009
- [7] G. Belingardi, D.S. Paolino, E.G. Koricho, Investigation of influence of tab types on tensile strength of E-glass/epoxy fiber reinforced composite materials, *Procedia engineering*, 2011, vol. 10 n. ICM11, pp. 3279-3284.
- [8] P. B. S. Bailey, A. D. Lafferty, Specimen gripping effects in composites fatigue testing - Concerns from initial investigation, *eXPRESS Polymer Letters* Vol.9, No.5 (2015) 480–488.
- [9] M. Levesque, L'essai de traction de matériaux composites unidirectionnels à fibres continues, Master Thesis, École polytechnique de Montréal, 2000.
- [10] A. R. Bunsell, A. Somer, The tensile and fatigue behaviour of carbon fibers, *Plastics Rubber and Composites Processing and Applications*, 1992, 18(4), 263-267.
- [11] A.E. Scott, I. Sinclair, S.M. Spearing, A. Thionnet, A.R. Bunsell, Damage accumulation in a carbon/epoxy composite: Comparison between a multiscale model and computed tomography experimental results, *Composites Part A: Applied Science and Manufacturing*, Volume 43, Issue 9, September 2012, Pages 1514-1522.
- [12] C. Huchette, Sur la complémentarité des approches expérimentales et numériques pour la modélisation des mécanismes d'endommagement des composites stratifiés, PhD Thesis, 2005, ONERA-Université Paris 6.
- [13] F. Laurin, Approche multi-échelle des mécanismes de ruine progressive des matériaux stratifiés et analyse de la tenue de structures composites, PhD thesis, 2005, ONERA-Université de Franche-Comté.